THYROID
Volume 30, Number 2, 2020
© Mary Ann Liebert, Inc.
DOI: 10.1089/thy.2019.0598

Generation of Novel Genetic Models to Dissect Resistance to Thyroid Hormone Receptor α in Zebrafish

Cho Rong Han,[1] Erik Holmsen,[1] Blake Carrington,[2] Kevin Bishop,[2] Yuelin Jack Zhu,[3] Matthew Starost,[4] Paul Meltzer,[3] Raman Sood,[2] Paul Liu,[2] and Sheue-yann Cheng[1]

Background: Patients with mutations of the thyroid hormone receptor alpha (*THRA*) gene show resistance to thyroid hormone alpha (RTHα). No amendable mouse models are currently available to elucidate deleterious effects of TRα1 mutants during early development. Zebrafish with transient suppressed expression by morpholino knockdown and ectopic expression of TRα1 mutants in the embryos have been reported. However, zebrafish with germline transmittable mutations have not been reported. The stable expression of *thra* mutants from embryos to adulthood facilitated the study of molecular actions of TRα1 mutants during development.
Methods: In contrast to human and mice, the *thra* gene is duplicated in zebrafish, *thraa*, and *thrab*. Using CRISPR/Cas9-mediated targeted mutagenesis, we created dominant negative mutations in the two duplicated *thra* genes. We comprehensively analyzed the molecular and phenotypic characteristics of mutant fish during development.
Results: Adult and juvenile homozygous *thrab 1-bp ins (m/m)* mutants exhibited severe growth retardation, but adult homozygous *thraa 8-bp ins (m/m)* mutants had very mild growth impairment. Expression of the growth hormone (*gh1*) and insulin-like growth factor 1 was markedly suppressed in homozygous *thrab 1-bp ins (m/m)* mutants. Decreased messenger RNA and protein levels of triiodothyronine-regulated keratin genes and inhibited keratinocyte proliferation resulted in hypoplasia of the epidermis in adult and juvenile homozygous *thrab 1-bp ins (m/m)* mutants, but not homozygous *thraa 8-bp ins (m/m)* mutants. RNA-seq analysis showed that homozygous *thrab 1-bp ins (m/m)* mutation had global impact on the functions of the adult pituitary. However, no morphological defects nor any changes in the expression of *gh1* and keratin genes were observed in the embryos and early larvae. Thus, mutations of either the *thraa* or *thrab* gene did not affect initiation of embryogenesis. But the mutation of the *thrab* gene, but not the *thraa* gene, is detrimental in postlarval growth and skin development.
Conclusions: The *thra* duplicated genes are essential to control temporal coordination in postlarval growth and development in a tissue-specific manner. We uncovered novel functions of the duplicated *thra* genes in zebrafish in development. These mutant zebrafish could be used as a model for further analysis of TRα1 mutant actions and for rapid screening of therapeutics for RTHα.

Keywords: zebrafish, TRα mutations, growth retardation, epidermis hypoplasia, pituitary defects, RNA-seq

Introduction

Thyroid hormone nuclear receptors (TRs) are transcription factors that mediate the biological activities of the thyroid hormone triiodothyronine (T3). In humans, the two TR genes, thyroid hormone receptor alpha (*THRA*) and thyroid hormone receptor beta (*THRB*), encode TRα1 and TRβ, respectively. Given the critical roles of TR in growth, differentiation, and development, mutations of the TR genes are deleterious, resulting in diseases. In the late 1980s, mutation of the *THRB* gene was reported to cause a genetic disease known as resistance to thyroid hormone (RTH)β with hallmarks of dysregulation of the pituitary–thyroid axis (1). However, no patients with mutation of the *THRA* gene were discovered until 2012–2013 (2–4). The patients reported so far were found to have the mutation sites clustered at the

[1]Laboratory of Molecular Biology, National Cancer Institute, National Institutes of Health, Bethesda, Maryland.
[2]Zebrafish Core, Translational and Functional Genomics Branch, National Human Genome Research Institute, National Institutes of Health, Bethesda, Maryland.
[3]Laboratory of Genetics, National Cancer Institute, National Institutes of Health, Bethesda, Maryland.
[4]Division of Veterinary Resources, Diagnostic and Research Services Branch, National Institutes of Health, Bethesda, Maryland.

C-terminal region of the T3-binding domain (2–6). Many mutations are frameshift mutations, ending with truncations, with amino acids shorter than the wild-type (WT) TRα1. Patients have a slightly higher T3 and lower L-thyroxine (T4), but the thyrotropin (TSH) is mostly normal, or mildly elevated. However, patients show RTHα by exhibiting debilitating symptoms of growth retardation, delayed bone development, neurological abnormalities, cognitive defects, and anemia (2–6). The molecular basis underlying these disorders has yet to be fully elucidated.

Our laboratory previously created a mouse model (*Thra1*$^{PV/+}$ mice) to elucidate the *in vivo* pathogenic actions of TRα1 mutants (7). *Thra1*$^{PV/+}$ mice express a mutant TRα1, known as PV, which has a C-terminal frameshift mutated sequence similar to the mutant TRα1 identified in two patients. The *Thra1*$^{PV/+}$ mouse faithfully reproduces growth retardation (7), delayed bone development (8,9), and anemia (10) as reported for patients. While much has been learned about the molecular actions of TRα1PV mutants from using adult *Thra1*$^{PV/+}$ mice, little is known about how these mutants exert their deleterious effects during early development. This is because of the difficulty in obtaining sufficient embryos at the early stage of development in *Thra1*$^{PV/+}$ mice. The fertility of *Thra1*$^{PV/+}$ mice is severely deficient, yielding a very small litter size with only two or three pups, frequently with no pups having the *Thra1*^{PV} mice genotype. Clearly, alternative animal models that can mitigate these shortcomings are needed.

We chose zebrafish (*Danio rerio*) to study the molecular actions of TRα in development because zebrafish have high fecundity, rapid external embryonic development, and easy visualization of transparent embryos. The zebrafish has two duplicated *thra* genes, the *thraa* and *thrab* genes. The *thraa* gene encodes two TRα1 isoforms, the short (TRα1S) and the long form with an additional 14 amino acids at the C-terminus (TRα1L). The *thrab* gene encodes one single TRαB receptor. The DNA- and T3-binding domains of TRα1S, TRα1L, and TRαB share 90–95% sequence homology with the human and mouse TRα1 (11,12). The effects of transient suppressed expression of the *thraa* gene on the embryonic development and larva transition in zebrafish were reported by morpholino knockdown (13). The functional consequences of ectopic expression of several human TRα1 mutants in zebrafish embryos have been evaluated (14). However, in contrast to these studies in which the effects were transient, we aimed to generate novel zebrafish RTHα models in which the mutations are germline transmittable with stable expression of TRα1 mutants controlled by endogenous promoters and transcription regulatory mechanisms. Such stable gene expression will allow us to assess the molecular actions of TRα1 mutants from the embryonic stage to adulthood.

In this study, we report the generation of zebrafish *thraa* and *thrab* mutants with C-terminal truncation mutations similar to those found in human RTHα patients. No discernible embryonic defects were detected in fish expressing either *thraa* or *thrab* mutations. However, both the *thraa* and *thrab* mutations caused growth retardation as in patients, with a stronger deleterious effect induced by the *thrab* mutant. The onset of the impaired growth occurred during the larva–juvenile transition, when thyroid hormones were at their peak. Furthermore, the *thrab* mutant, but not the *thraa* mutant, caused a hypoplastic epidermis and aplastic musculature, beginning at the larva–juvenile transition and persisting to adults. Thus, the fact that the duplicated genes evoke differential responses suggested the *thrab* gene product, the TRαB receptor, plays a predominant role during postembryonic/larval development. Furthermore, the retarded growth commonly observed in *thra* mutant fish, as in humans and mice, indicates that the deleterious effects of mutations of TRα are conserved from mammals to teleost fish.

Materials and Methods

Ethics statement

All zebrafish experiments were performed in compliance with the guidelines for animal handling and approved animal study protocols under the National Cancer Institute's and the National Human Genome Research Institute's Animal Care and Use Committees.

Zebrafish husbandry

The zebrafish mutant lines in the TAB5 background were used for studies. Zebrafish embryos were collected by natural crosses for each *thra* mutant line using heterozygous adults and staged according to hours or days postfertilization (hpf or dpf) as described (15). In all cases, fish were anesthetized in MS222 before an experiment began. Mutant fish after F4 generation were used in the phenotypic characterization.

Generation of thraa *and* thrab *mutant fish and genotyping*

Single guide RNAs (sgRNAs) targeting *thraa* (Ensembl transcript ID: ENSDART00000000160.10) exon 9 (GgTCC CGCCGCTCTTCCTGG) and *thrab* (Ensembl transcript ID: ENSDART00000153187.2) exon 10 (GgGGGGGAAAGAG TTCAGTG) were designed using the ''ZebrafishGenomics'' track on the UCSC Genome Browser. Synthesis of target oligonucleotides (Integrated DNA Technologies), preparation of messenger RNA (mRNA), microinjections, evaluation of sgRNA activities by CRISPR-STAT, and generation of mutant lines were carried out as described previously (16). In brief, WT embryos (TAB5) were injected with sgRNAs (50 pg) and Cas9 mRNA (300 pg) and grown to adulthood. Screening for germline transmission of indels was carried out by analysis of eight embryos from the progeny of each founder fish at 24 hpf by fluorescent PCR using the following primer sets: thraa-E9-Forward (5′-TCT GGACTGACATGTGTGG) and thraa-E9-Reverse (5′-TTT TGCCGCTGTGTCTCTGG); thrab-E10-Forward (5′-CTAC ATCAACTATCGCAAGC), and thrab-E10-Reverse (5′-AC GTTCCTGATTCTCTTGCC). A M13F adapter (5′-TGTA AAACGACGGCCAGT) was added to the 5′ end of each forward primer, and a PIG-tail (5′-GTGTCTT) was added to the 5′ end of each reverse primer as described (17). Progeny of founder fish for selected mutations were grown to adulthood and genotyped by fluorescent PCR followed by sequencing to determine its predicted effect on the encoded protein. The same primer sets were used for all subsequent genotyping of embryos and adults during phenotype analysis of the mutant fish.

Analysis of body length, width, and weight of zebrafish

Mutant fish of the same cohort that were growing together were used in the analysis of body length, width, and weight. The larval fish at 14–15 dpf, juvenile fish at 1 month postfertilization (mpf), and adult fish at 3–6 mpf were euthanized and we performed standard body length (centimeters) and width (centimeters) measurements using digital calipers (VWR international) and weighed (grams) (Mettler Toledo XS64). They were genotyped by tissue collection for larval and juvenile fish, and by fin clipping for adult fish as described earlier. Body length, width, and weight data were grouped based on their genotype and statistical analyses were performed using GraphPad Prism 7.7 software (GraphPad Software, Inc.). For statistical tests, two-tail unpaired *t*-test were used (p-adjusted <0.05).

Zebrafish sample collection

Fish were euthanized with MS222 before all tissue collections. For RNA-seq analysis, zebrafish pituitaries were isolated from WT (triplicates, pooled pituitaries from 10 to 12 fish for each run) and homozygous *thrab 1-bp insertion (m/m)* mutant adult females (quadruplicates, pooled pituitaries from 10 to 12 fish for each run). The age of fish was 4.5–5.7 mpf. For real-time quantitative PCR (RT-qPCR) analysis, ∼85 pituitaries were obtained from juveniles at 1 mpf and from adult male and female zebrafish at 3–6 mpf. Muscle tissues were collected by transecting the fish from the anterior border of the anal fin to the posterior border of the dorsal fin, excluding the fins themselves. The skin on the belly of fish was collected by transecting the fish from the pectoral fin to the anal fin, without muscle, digestive organs, and fins. The skin on the belly was collected from female zebrafish (4.9 mpf), from both female and male juveniles (1 mpf), and from larvae at 14 or 15 dpf. In all cases, sample collection was performed with a LEICA GZ4 microscope.

Histological analyses

Zebrafish were euthanized and fixed in 4% formaldehyde at 4°C for a minimum of 24 hours followed by decalcification in 1:1 ratio formic acid/sodium citrate for 24 hours at room temperature. The fish were then dehydrated through a series of ethanol, then xylenes, and finally embedded in paraffin. Five-micrometer sections were prepared and stained with hematoxylin and eosin (Histoserv, Germantown). Histological section images were captured with an Olympus BX41 light microscope.

Determination of whole-body content of total thyroid hormones in zebrafish

The concentrations of total T4 (TT4) and total T3 (TT3) were performed as described (18). To measure the concentrations of TT3 and TT4 by enzyme-linked immunosorbent assay (ELISA), larvae, juvenile, and adult fish were collected postfertilization of day 3, day 7, day 15, day 30, and 3 months. All samples were weighed and homogenized in methanol containing 1 mM 6-propyl-2-thiouracil (Sigma) on ice, then frozen at −80°C until used. Homogenized samples were centrifuged at $6723 \times g$ for 30 minutes at 4°C, supernatant was collected, dried by Speed Vac system (AES1010) for 7 hours, and resuspended in phosphate-buffered saline (PBS) for 24 hours at 4°C (body weight 0.6 g/250 μL PBS) and centrifuged at 14,000 rpm for 5 minutes at 4°C, after which the supernatants were collected for thyroid hormone measurements. Samples were analyzed using a T4 ELISA Kit (Cat. No. 3149-18; Diagnostic Automation) for TT4 concentration and T3 ELISA Kit (Cat. No. 3144-18; Diagnostic Automation) as indicated by the manufacturer's protocol. Standard curves, concentrations of TT3 and TT4 were calculated using online analysis software (www.elisanalysis.com). All standard curves showed $R^2 > 0.94$. Statistical analyses were performed using GraphPad Prism 7.7 software (GraphPad Software, Inc.). The number of fish used in the determination are as follows: 3 and 7 dpf larvae ($N = 800$–950 per sample, in triplicates), 15 dpf larvae ($N = 140$–180 per sample, in triplicates), 30 dpf juveniles ($N = 6$–9 per sample, in triplicates), and adult fish ($N = 3$ per sample in triplicates). To measure the relative concentration of TT3 and TT4 in 30 dpf juveniles between WT and homozygous *thrab 1-bp ins (m/m)* mutant fish, the number of fish used were in the range of 6–9, 20–31 per sample, each in triplicates for WT fish and 16–19 or 36 fish per sample, each in triplicates for mutant fish. For 100 dpf adult fish, the number of fish used were 3 per sample, each in triplicates for WT fish and 8–9 or 7–9 fish per sample, each in triplicates for homozygous *thrab 1-bp ins (m/m)* mutants.

Transcriptome analysis of the pituitary of female homozygous thrab 1-bp insertion *mutant fish*

The libraries were prepared according to the Illumina TruSeq mRNA Prep protocol for paired-end sequencing and then sequenced on an Illumina HiSeq 2500 sequencer. After confirmed good sequence quality, the raw reads of the samples were processed with common RNA-Seq processing procedure, including trimming reads for removing adapters and low-quality bases using Trimmomatic software, aligning with the reference genome (Ensembl GRCz11) using STAR aligner version 2.5.1. from Cold Spring Harbor Laboratory (PMID: 23104886), marking duplicated reads using Picard's MarkDuplicate utility, calculating raw read counts using RSEM software package version 1.2.22 from University of Wisconsin-Madison (19). Normalization and differential expression analysis between mutant and WT groups was done with edgeR Bioconductor package (20). Mainly, linear models (glmFit and glmLRT) were applied to the normalized counts and significant genes were selected by fold change ≥2 and false discovery rate (FDR) ≤0.05.

RNA isolation and RT-qPCR

Total RNA from pituitaries, tail muscle, and skin on the belly were isolated using TRIzol (Invitrogen) as indicated by the manufacturer's protocol. RT-qPCR was performed with one step SYBR Green RT-qPCR Master Mix (Qiagen, Valencia, CA) on an ABI 7900HT system. In each genotype, samples with triplicates were tested on the target genes. Data were analyzed using Prism 7.7 software (GraphPad Software, Inc.). For statistical tests, two-tail unpaired *t*-test were used (p-adjusted <0.05). Primer sequences are shown in Supplementary Table S1. *Ef1a* was used as the housekeeping gene for controls.

Western blot analysis

The Western blot analyses were performed as described (21). Primary antibodies for p-AKT (Ser-473) (Cat. No. 4060), AKT (Cat. No. 9272), p-p70S6 (Thr-389) (Cat. No. 9205), p70S6 (Cat. No. 9202), p-S6 (Ser-240/244) (Cat. No. 2215), S6 (Cat. No. 2217), p-STAT3 (Cat. No. 9131), STAT3 (Cat. No. 4904), p-Rb (Ser-780) (Cat. No. 9307), and GAPDH (Cat. No. 2118) were purchased from Cell Signaling Technology. The keratin-5 primary antibody (Cat. No. MS-1814-S0) and keratin-17 (Cat. No. MS-489-S0), keratin-18 (Cat. Nos. MS-743-S0 and MS-1850-S0), and cyclinD1 (Cat. No. 9041-P1) were purchased from NeoMakers (Fremont, CA). The primary antibody CDK6 (sc-7961) and Rb (sc-50) were purchased from Santa Cruz Biotechnology. Antibodies were used at the manufacturer's recommended concentration. For control of protein loading, the blot was probed with the antibody against GAPDH. The species specificity and other relevant information about the antibodies used in this study are listed in Supplementary Table S2.

Statistical analysis

All data are expressed as mean ± standard deviation. All tests were two-tail unpaired *t*-test and $p < 0.05$ was considered significant. GraphPad Prism version 7.7 for Mac OS X was used to perform analyses of variances.

Results

Generation of thraa *and* thrab *mutants by CRISPR/Cas9-mediated targeted mutagenesis*

The mutation sites identified in RTHα patients so far are all clustered at the C-terminus of TRα1 (22). In contrast to one single *THRA* gene in humans, zebrafish have duplicated *thra* genes: *thraa* and *thrab* (11,12,23). The *thraa* gene, located on chromosome 3, encodes two TRα1 receptors: the short form (TRα1S) and the long form (TRα1L). The *thrab* gene, located on chromosome 12, encodes one single receptor protein, TRαB. To model RTHα in zebrafish, we needed to mutate both the *thraa* and *thrab* genes. These two duplicated genes share 90–95% sequence homology in the functional DNA-binding and ligand-binding domains with the human *THRA* gene (11–13). We used CRISPR/Cas9-mediated targeted mutagenesis to generate four lines of mutant fish (Table 1). A 4-base pair (bp) deletion in exon 9 of the *thraa* gene (*thraa 4-bp del*) resulted in frame-shift truncated ThraaPhe404-Leufs*22 and ThraaPhe404Leufs*10, when aligned with the WT TRα1L or TRα1S, respectively (Table 1). An 8-bp insertion in the exon 9 of the *thraa* gene (*thraa 8-bp ins*) resulted in a single frame-shift truncated ThraaLeu405Glufs*6 protein when aligned with the WT TRα1L or TRα1S (Table 1). A 4-bp deletion or a 1-bp insertion in exon 9 of the *thrab* gene (*thrab 4-bp del* or *thrab 1-bp ins)* led to a frame-shift mutant ThrabThr393Profs*31 or a truncated ThrabGlu394*, respectively (Table 1).

Functional characterization of T3-binding (Supplementary Fig. S1; see Supplementary Materials and Methods) and transcriptional activity (Supplementary Fig. S2; see Supplementary Materials and Methods) showed that ThraaPhe404-Leufs*22, ThraaLeu405Glufs*6, and ThrabGlu394* had totally lost T3-binding activity and transcriptional capacity (Table 2). Moreover, these three mutants all exhibited strong dominant negative activity by interfering with the transcription activity of WT receptors (Supplementary Fig. S2; Table 2). However, to our surprise, we found that ThrabThr393Profs*31 derived from a 4-bp deletion in exon 9 of the *thrab* gene functioned as a WT receptor. This C-terminal frame-shift mutant with an additional 13 amino acids longer than TRαB receptor bound to T3 (Supplementary Fig. S1D; see Supplementary Materials and Methods) and exhibited transcriptional activity (Supplementary Fig. S2C; Table 2). On the basis of functional characteristics, we focused our studies on the fish lines derived from an 8-bp insertion of the *thraa* gene and a 1-bp insertion of the *thrab* gene that encoded ThraaLeu405Glufs*6 and ThrabGlu394*, respectively (Tables 1 and 2). The C-terminal truncation mutation in ThraaLeu405Glufs*6 is

Table 1. Comparison of the C-Terminal Amino Acid Sequences of Wild-Type and Mutant Thyroid Hormone Receptor α Generated Through CRISPR/CAS9-Mediated Targeted Mutagenesis

Protein	*C-terminal amino acid sequence*
The *thraa* gene	
Wild-type TRα1L	-FPPLFLEVFEDQEGSTGVAAQEDGSCLR*-428
4-bp deletion ThraaPhe404Leufs*22	-FPPL*LRSSRIRREALEWQHRKTVPA**-425
8-bp insertion ThraaLeu405Glufs*6	-FPPLF*EDQEV**-410
Wild-type TRα1S	-FPPLFLEVFEDQEV*-414
4-bp deletion ThraaPhe404Leufs*10	-FPPL*LRSSRIRRC**-412
8-bp insertion ThraaLeu405Glufs*6	-FPPLF*EDQEV**-410
The *thrab* gene	
Wild-type TRαB	-HASRFLHMKVECPTELFPPLFLEVFEDQDV*-409
4-bp deletion ThrabThr393Profs*31	-HASRFLHMKVECP*PSFPHFSWRSSRIRTCDVPANCGKRIRNVS**-422
1-bp insertion ThrabGlu394*	-HASRFLHMKVECPT*-394

bp, base pair.

Table 2. Summary of Functional Characteristics of Four Mutants

Genotypes	*Mutant proteins*	*T3 binding*	*Transcription activity*	*Dominant negative activity*
thraa 4-bp deletion	ThraaPhe404Leufs*22	No	No	Yes
thraa 8-bp insertion	ThraaLeu405Glufs*6	No	No	Yes
thrab 1-bp insertion	ThrabGlu394*	No	No	Yes
thrab 4-bp deletion	ThrabThr393Profs*31	Yes	Yes	No

T3, triiodothyronine.

similar to the truncation mutation identified in one patient (TRα1F397fs406X; Supplementary Fig. S3A; see Supplementary Materials and Methods) (3) and the truncation mutation in ThrabGlu394* is similar to the mutations identified in patients (TRα1E403X and TRα1C392X; Supplementary Fig. S3B; see Supplementary Materials and Methods) (2,5).

Differential growth regulatory functions of the thraa *and* thrab *genes*

In vitro studies have shown that the ThraaLeu405Glufs*6 mutant and the ThrabGlu394* mutant exhibit dominant negative effect by interfering with the transcription activity of WT TRα1 (Supplementary Fig. S2; Table 2). It is known that TRα1 mutants exerted their dominant negative effects by upregulating the negatively regulated genes such as the thyrotropin beta (*TSHβ*) subunit gene shown in mutant mice with TRα1R438C mutation (24). In humans, the pituitary responds to serum TSH levels through the pituitary–thyroid axis negative feedback loop. TSH consists of two subunits, α and β. The *TSHβ* subunit gene is a known thyroid hormone (T3)/TR negatively regulated gene. Mutations of TRα1 was expected to upregulate T3-negatively regulated gene (24). Indeed, we found that the *tshba* gene was upregulated in the pituitaries of male and female homozygous adult *thraa 8-bp insertion (m/m)* and *thrab 1-bp insertion (m/m)* mutant fish (Supplementary Fig. S4; see Supplementary Materials and Methods). Thus, the functions of both mutant receptors were validated in the two lines of mutant fish *in vivo*.

What caught our attention in adult fish was the growth retardation exhibited by homozygous *thrab 1-bp insertion (m/m)* mutant fish as shown in Figure 1A-b (females) and 1E-b (males). Both females and males showed decreased body length (Fig. 1B, F), body width (Fig. 1C, G), and body weight (Fig. 1D, H). Interestingly, male homozygous *thrab 1-bp insertion (m/m)* mutant fish showed a more severe growth retardation in that a greater reduction was detected in body length (43% reduction in males and 19% reduction in females; Fig. 1F, B), body width (42% reduction in males vs. 19% reduction in females; Fig. 1G, C), and body weight (48% reduction in males vs. 44% reduction in females; Fig. 1H, D). However, no significant changes were detected in heterozygous fish of either sex in the body length, width, and weight. These data indicate that the growth of males was more affected by the mutations of the *thrab* gene.

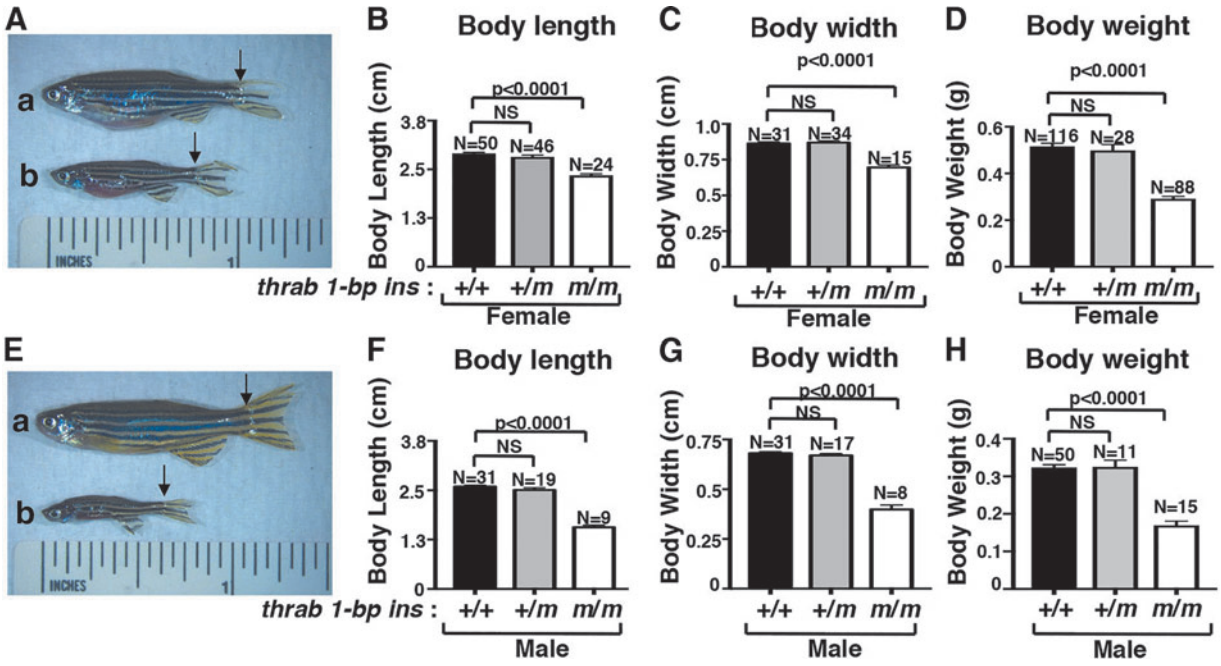

FIG. 1. Impaired growth in adult homozygous *thrab 1-bp insertion (m/m)* mutant fish. (**A**) Representative images of a female WT (**a**) and homozygous mutant fish (**b**) and (**E**) male fish (3.4 mpf) with black arrows to indicate the beginning of caudal fin used in the length measurements. Body length (**B**, **F**), body width (**C**, **G**), and body weight (**D**, **H**) were measured for both females and males of WT, heterozygous, and homozygous mutant fish. The number of fish (*N*) measured are indicated. The data are shown as mean ± SE with *p*-values to indicate significant changes. Two-tail unpaired *t*-test, *p*-adjusted <0.05 was used for statistical analysis. mpf, month postfertilization; NS, not significant; SE, standard error; WT, wild-type.

The homozygous *thraa 8-bp insertion (m/m)* mutant fish also exhibited retarded growth. However, the deleterious effect of the *thraa 8-bp insertion (m/m)* mutation on growth was much weaker than that of the *thrab 1-bp insertion (m/m)* mutation (Supplementary Fig. S5; see Supplementary Materials and Methods). Only small decreases in body length (~6%), body width (~6%), and body weight (~12%) were detected in homozygous male *thraa 8-bp insertion (m/m)* mutants, but not females (Supplementary Fig. S5). Thus, similar to *thrab 1-bp insertion (m/m)* mutants, there was a preponderance in males of growth defects in *thraa 8-bp insertion (m/m)* mutants. Since the *thraa 8-bp insertion (m/m)* mutants exhibits very mild growth abnormalities, we focused our studies on the molecular actions of the *thrab 1-bp insertion (m/m)*. We analyzed the expression of growth-related genes in the pituitary to understand how the *thrab 1-bp insertion (m/m)* mutant led to growth retardation. The growth hormone (*gh*) gene is a direct T3/TR target gene (25–27). Figure 2A shows that the expression of the *gh1* gene was reduced (77%), as was the growth hormone-related *smtl* gene (28,29) (*smtla* and *smtlb* had 99% and 92% reduction, respectively). It is of interest to note that the expression of *smtla* and *smtlb* was similarly suppressed in the pituitary of the *thraa 8-bp insertion (m/m)* mutation fish as in *thrab 1-bp insertion (m/m)* mutant fish. However, the expression of the *gh1* gene was not suppressed, but elevated, in the *thraa 8-bp insertion (m/m)* mutation fish (Supplementary Fig. S6; see Supplementary Materials and Methods).

The growth-promoting effects of the GH are mainly mediated by insulin-like growth factor 1 (IGF-1) signaling. GH stimulates the synthesis of IGF-1 in the muscles (30). IGF-1 increases muscle mass mainly through IGF-1 receptors and also through insulin receptor (Ir). Since it is known that fish growth is primarily dependent on an increase in muscle mass (31), we analyzed the IGF actions in the muscle. We found *igf-1a* and *-1b* mRNA was reduced (39–49%). However, the expression of the *Igf-1ra* and *Igf-1rb* genes was not affected. But the expression of the *Ir-a* and *glut4* genes was decreased (78% and 51%, respectively; Fig. 2A-II). However, myostatin (*myo*), which acts as a negative regulator of the GH (32), was not changed in its expression (Fig. 2A-II) such that it did not further affect the *gh1* expression.

We next analyzed the IGF-1 downstream AKT-p70S6 pathway (30,33). The activity of AKT was reduced as

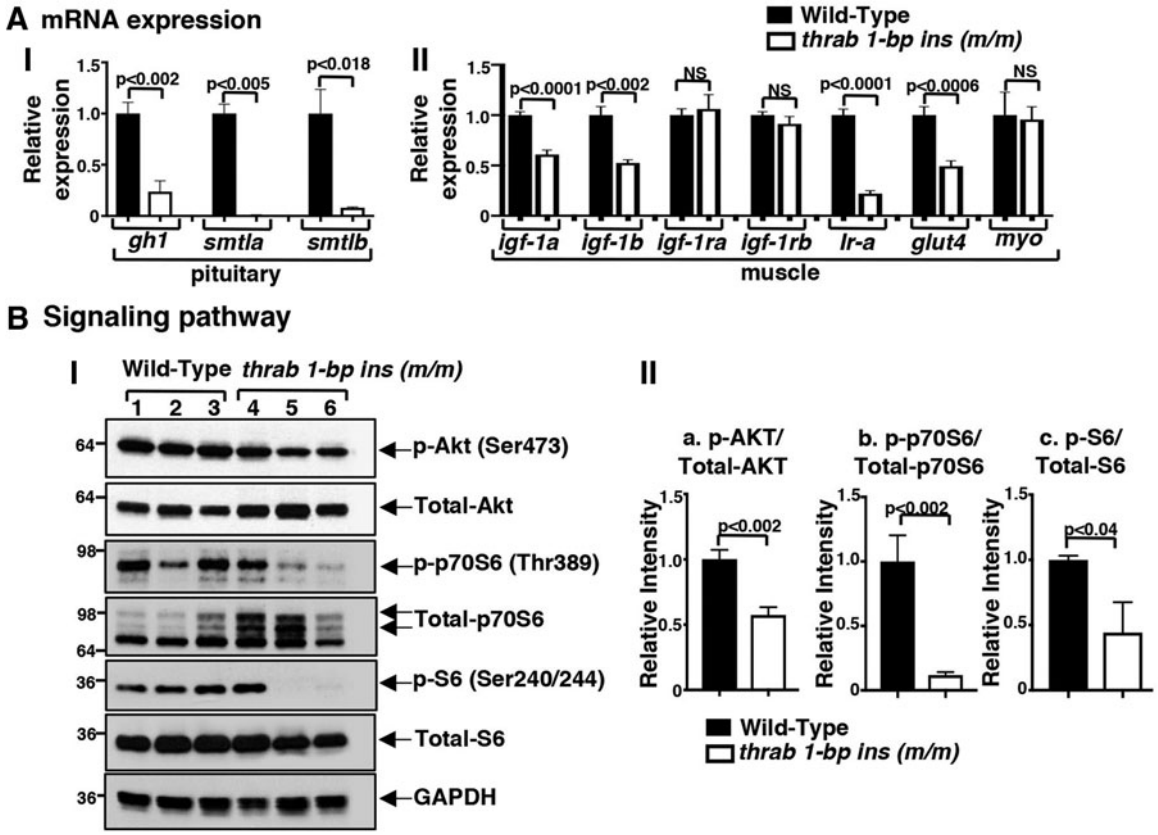

FIG. 2. Altered gene expression (**A**) and key regulatory proteins in growth signaling pathway (**B**) in adult female homozygous *thrab 1-bp insertion (m/m)* mutant fish. The mRNA expression of *gh1*, *smtla*, and *smtlb* in pituitary (**A-I**) and mRNA expression of *igf-1a*, *igf-1b*, *igf-1ra*, *igf-1rb*, *Ir-a*, *glut4*, and *myo* in the muscles (**A-II**) of WT (solid bars) and sibling homozygous *thrab 1-bp insertion (m/m)* mutant fish (open bars) were determined by RT-PCR as described in Materials and Methods section. Number of fish = 10–15 for pituitaries, 5–3 for muscles. (**B-I**) Western blot analysis was carried out for p-AKT (Ser473), total AKT, p-p70S6 (Thr389), total p70S6, p-S6 (Ser240/244), total S6, and GAPDH, using muscle as described in Materials and Methods section. (**B-II**) Quantitative analysis of relative protein expression levels of the ratios of p-AKT to total AKT (**a**), p-p70S6 to total p70S6 (**b**), and p-S6 to total S6 (**c**) using GAPDH as a loading control. The data are shown as mean ± SE ($n = 3$; the p-values are indicated). Two-tail unpaired t-test, p-adjusted <0.05 was used for statistical analysis. mRNA, messenger RNA; RT-PCR, real-time PCR.

indicated by the decreased abundance of p-AKT (Fig. 2B-I, B-II, panel a), leading to decreased phosphorylation of p70S6 and 40S ribosomal protein S6 (Fig. 2B-I), a major component of the machinery involved in protein synthesis. Quantitation data show a 56–88% reduction in the ratios of p-p70S6/total p70S6 and p-S6/total S6 (Fig. 2B-II, panels b and c). Taken together, these data indicate that the homozygous *thrab 1-bp insertion (m/m)* mutant could reduce growth through decreasing IGF-1 signaling in the zebrafish. These findings are consistent with those reported in RTHα patients in that serum IGF-1 was decreased (2,22,34,35).

We next asked how early in development the homozygous *thrab 1-bp insertion (m/m)* mutant exerts its deleterious effects. We evaluated the growth characteristics of juveniles at 28 dpf (Fig. 3A). The body length was decreased by 15% (Fig. 3A-I, panel a), body width by 21% (panel b), and weight by 49% (panel c) in homozygous ThrabGlu394* juveniles as compared with WT siblings. No significant changes in growth characteristics were detected in the heterozygous juveniles. Gene expression analysis showed that the expression of the *gh1*, *smtla*, and *smtlb* genes was decreased 67%, 72%, and 60%, respectively, as compared with WT siblings (Fig. 3A-II). Interestingly, in larvae at the earlier age of 14–15 dpf, no apparent growth defects or altered expression of growth-related genes were detected (Fig. 3B-I, B-II).

Homozygous thrab 1-bp insertion (m/m) *mutant fish exhibit a hypoplastic epidermis and aplastic musculature*

Adult homozygous *thrab 1-bp insertion (m/m)* mutant fish showed the appearance of a bulging ''red belly,'' as indicated by arrows in Figure 4A-b (also visible in the mutant fish shown in Fig. 1A-b and E-b). Supplementary Figure S7 (see Supplementary Materials and Methods) shows an enlarged image of a homozygous *thrab 1-bp insertion (m/m)* mutant fish with clearly visible ''red belly.'' Analysis of WT skin showed normal epidermis, scales, and abdominal wall (Fig. 4B-a, female, and B-c, male). However, in the homozygous *thrab 1-bp insertion (m/m)* mutant fish, the ventral body wall musculature was thinned or absent in serial sections with only thin skin separating the heart, liver, and intestinal tract from the environment (Fig. 4B-b, B-d). The mutant fish had both hypoplasia (thinning) of the epidermis and aplasia (lack) of scales, and the ventral body wall musculature was hypoplastic to aplastic (for comparison see panels b and d with panels a and c, Fig. 4B). The thinning/loss of these structures led to the fish being more transparent, thus allowing the internal organs to be visible more clearly with the appearance of having reddening of the gill/body cavity (''red belly''; Fig. 4A-b). The scales are present, but in fewer numbers and of smaller size than in WT zebrafish.

It is generally recognized that thyroid hormone signaling is central to maintaining skin homeostasis. In humans, thyroid dysfunction is associated with alterations in skin architecture and physiology (36). The fact that homozygous *thrab 1-bp insertion (m/m)* mutant fish display a hypoplastic epidermis provides a model to understand the actions of TRα1 mutants in the skin. The majority of cell types in the epidermis are keratinocytes that express keratins. We determined the mRNA expression of keratin-related genes that are known to be regulated by thyroid hormones/TRs (37). Figure 5A shows that the expressions of *krt4*, *krt5*, *krt15*, *krt17*, *krt18*, *colla1b*, *cyt1*, and *cki* were all suppressed in the range of 49% (*colla1b*) to 92% (*cki*) in the skin of homozygous *thrab 1-bp insertion (m/m)* mutant fish. Consistent with the reduced

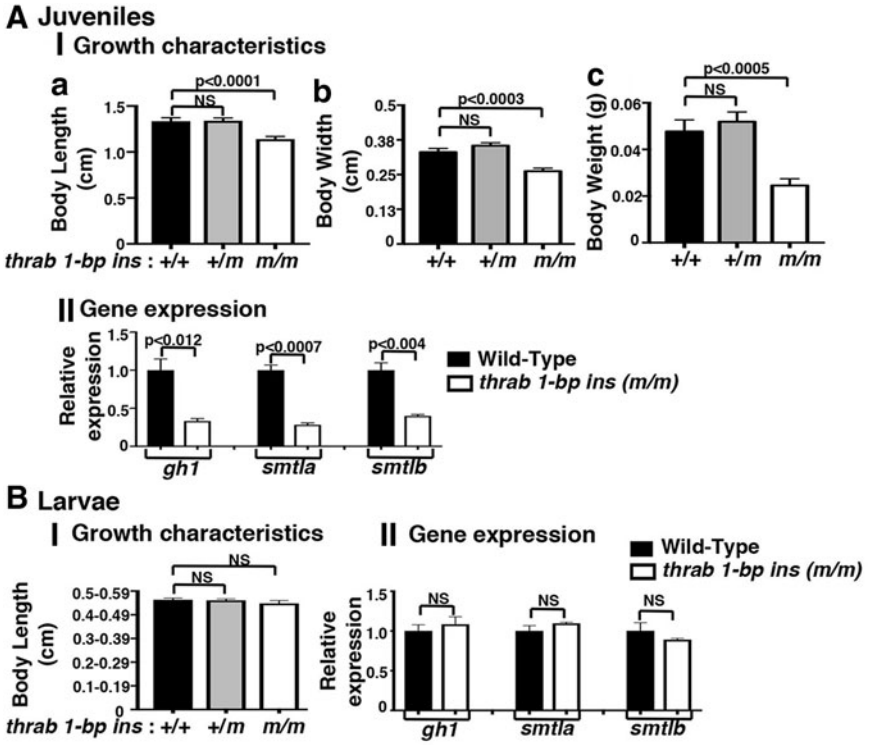

FIG. 3. Impaired growth occurred at larva to juvenile transitory phase of homozygous *thrab 1-bp insertion (m/m)* mutant fish. (**A**) Growth characteristics and gene expression of *thrab 1-bp ins* mutant fish for juveniles (28 dpf) and (**B**) larvae (15 dpf). Body length (**a**), body width (**b**), and body weight (**c**) were measured for juveniles (**A-I**) (number of fish = 22–29) and for larvae (**B-I**) (number of fish = 23–71). Relative mRNA expression of *gh1*, *smtla*, and *smtlb* was determined through RT-qPCR using the primers listed in Supplementary Table S1 for juveniles in the pituitary (**A-II**) and for larvae in head (**B-II**). The genotypes are indicated. The data are expressed as mean ± SE ($n = 3$; the p-values are indicated). Two-tail unpaired t-test, p-adjusted <0.05. dpf, days postfertilization; RT-qPCR, real-time quantitative PCR.

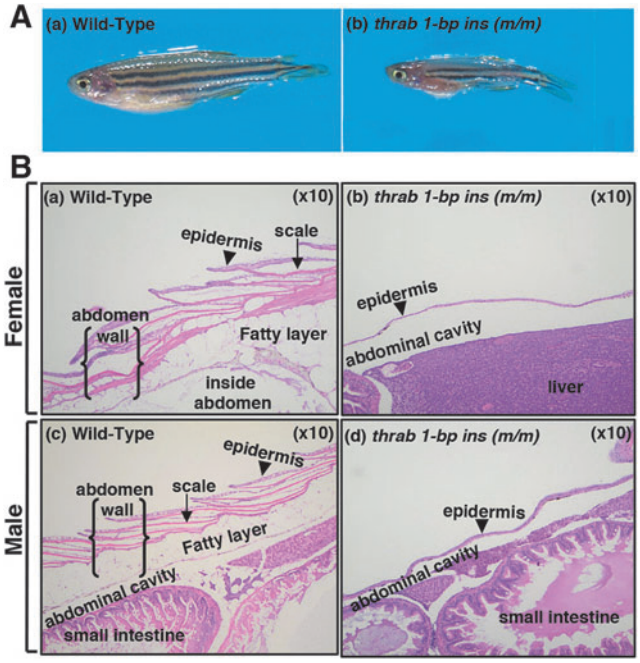

FIG. 4. Adult homozygous *thrab 1-bp insertion (m/m)* mutant fish exhibit hypoplastic epidermis and aplastic musculatures. (**A**) Representative images of WT fish (**a**) and homozygous *thrab 1-bp insertion (m/m)* mutant fish (**b**) with arrows marking the thin and red belly (denoted as ''red belly''). (**B**) Histology features of hematoxylin and eosin stained adult skin on the belly of WT female (**a**) and male (**c**) fish, and female homozygous *thrab 1-bp insertion (m/m)* mutant fish (**b**) and male (**d**) fish (10×objective). The arrow heads point to epidermis. Homozygous *thrab 1-bp insertion (m/m)* mutant fish of both sexes show very thin epidermis, lack of scales, and a true abdominal wall.

mRNA expression, the protein levels of keratin 5 (Fig. 5B-I, panel a), keratin 17 (panel b), and keratin 18 (panel c) were also decreased, ranging from 24% to 49% (see quantitation in Fig. 5B-II, panels a–c).

The hypoplastic epidermis suggested that proliferation of epidermal cells was inhibited in homozygous *thrab 1-bp insertion (m/m)* mutant fish. We searched for key cellular regulators that play critical roles in the proliferation of epidermal cells. Signal transducer and activator of transcription 3 (Stat3), upon activation by phosphorylation in the cytoplasm, enters into the nucleus to bind to DNA to stimulate transcription of target genes involved in cell proliferation, survival, migration, and oncogenesis (38,39). Stat3 has been reported to contribute to skin wound healing and keratinocyte migration (40). We, therefore, compared the Stat3 protein levels between WT and homozygous *thrab 1-bp insertion (m/m)* mutant fish. We found that p-Stat3(Tyr705) levels were markedly lowered in the mutant fish than the WT fish (lane 3 vs. lanes 1 and 2; Fig. 5C-I, panel a). After quantification of the intensities of the bands, the ratio of p-Stat3 versus total Stat3 in mutant fish was found to be reduced by 86% as compared with the WT (Fig. 5C-II, panel a). Cyclin D1, a key cell cycle regulator, is a known Stat3 downstream target gene (41). The protein levels of cyclin D1 together with another key cell cycle regulator, CDK6, were decreased by 64% and 38%, respectively, in the homozygous *thrab 1-bp insertion (m/m)* mutant fish (lane 3 vs. lanes 1 and 2; Fig. 5C-I, panels c and d, respectively; quantitation, Fig. 5C-II, panels b and c). Decreased cyclin D1/CDK6 led to decreased phosphorylation of retinoblastoma (Rb) (Fig. 5C-I, panel e; the ratios of p-Rb vs. total Rb was 89% lower in mutant fish than WT, Fig. 5C-II, panel d) to delay the cell cycle progression in the epidermis of homozygous *thrab 1-bp insertion (m/m)* mutant fish.

We next ascertained how early the thinning of the epidermis (''red belly'') became visible. We found that the thinning of the epidermis was apparent as early as 28 dpf. Analysis of the skin of juveniles shows that except *krt17*, the expression of the keratin-related genes was similarly suppressed (Fig. 6B). These results indicate that the homozygous *thrab 1-bp insertion (m/m)* mutant acts to suppress these keratin genes, leading to visibly defective epidermis as early as 28 dpf. While the ''red belly'' was not detectable in the larvae, gene expression indicates that the expression of *krt4*, *krt5*, and *krt15* is partially suppressed, but this is not the case for *krt7*, *krt18*, *colla1b*, *cyt1*, and *cki* (Fig. 6A), suggesting that partial suppression of the three *krt* genes (i.e., *krt4*, *krt5*, and *krt15)* is not sufficient to result in the hypoplastic phenotype on dpf 28.

Temporal expression of the thra *and* thrb *genes and thyroid hormone levels during zebrafish development*

The observations that homozygous *thrab 1-bp insertion (m/m)* mutation exhibit growth and skin abnormalities beginning at the larva–juvenile transition prompted us to ascertain the temporal expression of *thra* and *thrb* gene expression. Figure 7A shows that the expression of the *thrab*, *thraa*, and *thrb* genes is detectable after 1 dpf and gradually increases to day 5, with *thrab* reaching the highest level among the three genes. Figure 7B shows that the expression of these three genes continues to increase from 7 dpf larvae, reaching higher levels in adulthood.

We further determined TT4 and TT3 from embryos at 3 dpf, larvae at 7 dpf, and 15 dpf, juveniles at 30 dpf and adults (100 dpf). Figure 7B shows that TT3 and TT4 were barely detectable until 15 dpf, at which time, TT4 and TT3 began to rise, reaching a peak at juvenile age (30 dpf). Shortly after 30 dpf, both TT4 and TT3 slowly decrease. These findings are consistent with the observations that in WT mice, serum TT3 and TT4 are not detectable on the day of birth and rise to reach a peak on P15 (42). Figure 7C shows that TT3 and TT4 were 1.7- to 2.5-fold higher in homozygous *thrab 1-bp insertion (m/m)* mutant than WT fish in juveniles and in adults.

The homozygous thrab 1-bp insertion (m/m) *mutation has broad impact on the biology and functions of the pituitary*

Because the expression of *gh1*, *smtla*, and *smtlb* genes in the pituitary is affected by the homozygous *thrab 1-bp insertion (m/m)* mutant prompted us to further probe how mutations of the *thrab* gene could affect the expression of other genes in the pituitary. We, therefore, isolated the pituitaries from adult female fish and compared the global gene expression profiles in the pituitary between WT and

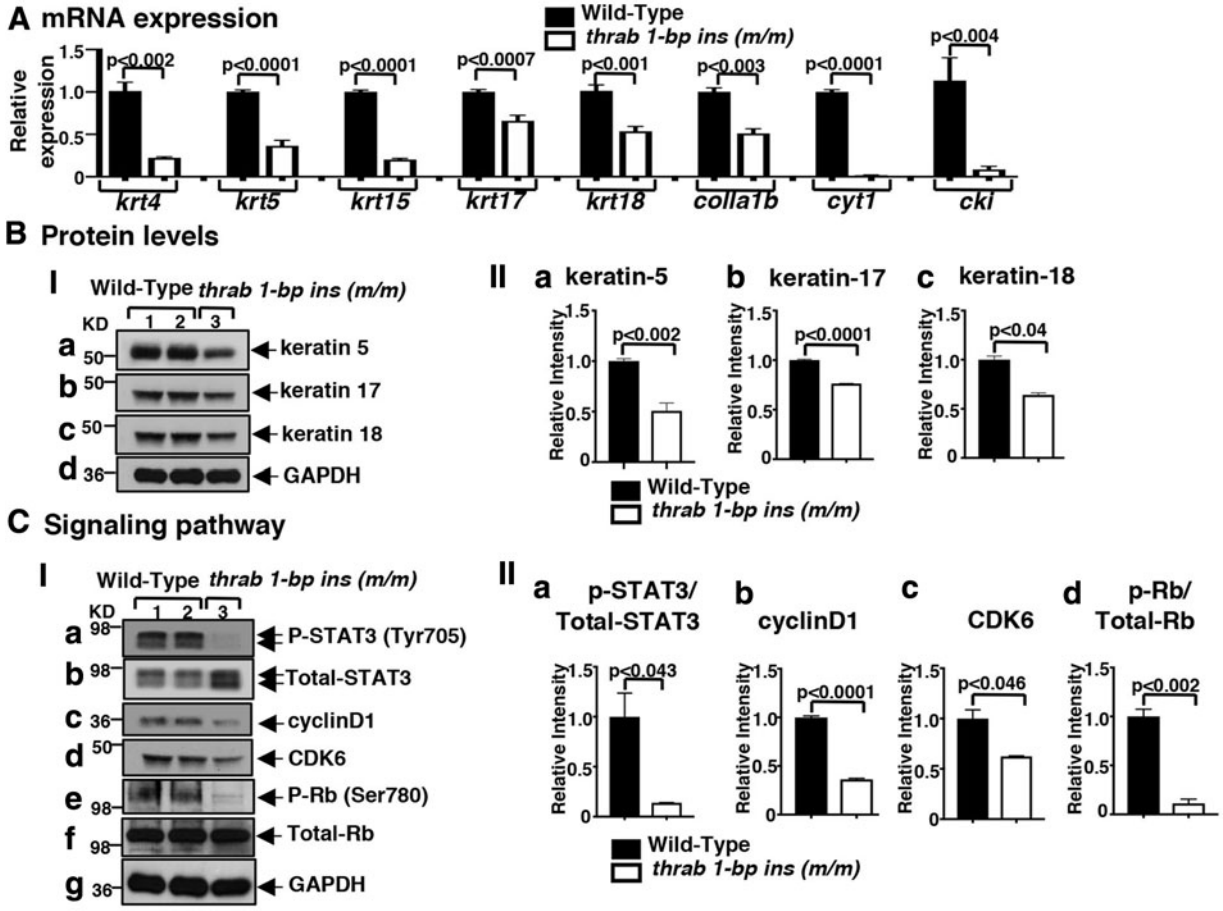

FIG. 5. Decreased keratin gene expression (**A**), protein abundance (**B**), and attenuated STAT3 signaling pathway (**C**) in the skin of adult homozygous *thrab 1-bp insertion (m/m)* mutant fish. (**A**) The expression of keratin genes (*krt4*, *krt5*, *krt15*, *krt17*, and *krt18)* and skin-regulated genes *(col1a1b*, *cyt1*, and *cki*) from the belly skin of fish with genotypes indicated was determined by RT-qPCR as described in Materials and Methods section (number of fish = 22–25). (**B-I**) Total protein extracts were prepared from skin on the belly and Western blot analysis for keratin-5, -17, -18 and GAPDH as described in Materials and Methods section. (**B-II**) Quantitative analysis of relative protein abundance of keratin-5 (**a**), keratin-17 (**b**), and keratin-18 (**c**) from the belly skin of fish with genotypes indicated (number of fish = 10). (**C-I**) Western blot analysis of p-STAT3 (Tyr705), total STAT3, and downstream STAT3 target proteins [cyclinD1, CDK6, p-Rb (Ser 780), total-Rb] and GAPDH from the belly skin of fish with genotypes indicated. (**C-II**) Quantitative analysis of relative protein expression levels of the ratio of p-STAT3 to total STAT3 (**a**), p-Rb to total Rb (**d**), and relative level of cyclin D1 (**b**) and CDK6 (**c**) using GAPDH as a loading control (number of fish = 10). The data are expressed as mean ± SE ($n = 3$–6; the p-values are indicated). Two-tail unpaired t-test, p-adjusted <0.05 was used for statistical analysis.

homozygous *thrab 1-bp insertion (m/m)* mutant fish by RNA-seq. The number of genes differentially expressed with more than twofold changes (with FDR <0.05) was 723 (marked in red in this volcano plot; Fig. 8A). Interestingly, 85% of these differentially expressed genes were upregulated ($n = 642$), and only 15% were downregulated ($n = 81$). Hierarchical clustering of the top 50 differentially expressed genes clearly showed that the gene expression patterns in the pituitary of WT and mutant fish were clearly distinct (Fig. 8B). Figure 8C shows the major pituitary hormones identified by RNA-seq with FDR <0.05 (Supplementary Table S3; see Supplementary Materials and Methods). The expression of *smtlb*, *gh1*, *pomca*, and *lhb* were downregulated and the expression of *tshba* and *trhrb* were upregulated (Fig. 8C). We validated the changes in the expression of six genes by RT-qPCR (Fig. 8D). The results were found to be in total agreement with the RNA-seq data. Using RT/qPCR, we also found that the *thraa*, *thrab*, and *thrb* genes were all expressed in the pituitary of WT fish (Supplementary Fig. S8; see Supplementary Materials and Methods). We found that *thraa* mRNA was more abundantly expressed than *thrab* mRNA. Consistent with reports by others, we also found that *thrb* mRNA is the major TR isoform expressed in the pituitary (Supplementary Fig. S8).

Further Gene Ontology analysis of the differentially expressed genes identified the top 10 clusters of biological processes as shown in Figure 8E. These biological processes were involved in skin development and function, organ development, cell signaling, cellular assembly, and protein synthesis, endocrine system development and function, cellular growth and proliferation, and developmental disorders. The changes in biological processes were mostly affected by the known TRα1 upregulated genes. The Gene Ontology analysis suggested that the homozygous mutation of the *thrab* gene has broad impact on the biology and functions of the pituitary, as exemplified by decreased GH synthesis, resulting in retarded growth.

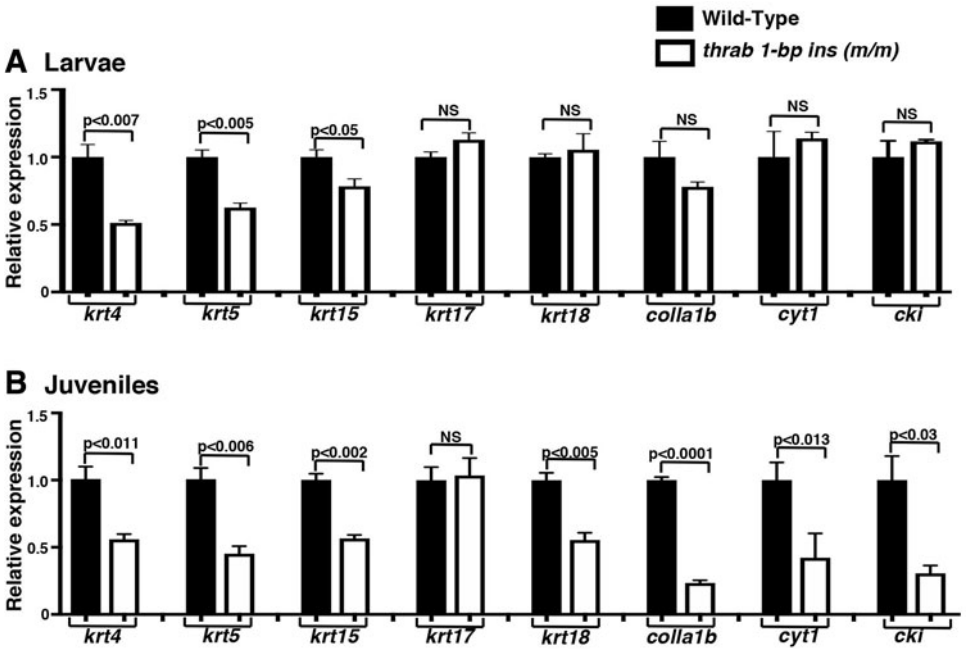

FIG. 6. Suppression of keratin expression program occurs during larva to juvenile transitory phase of homozygous *thrab 1-bp insertion (m/m)* mutant fish. (**A**) The expression of keratin genes (*krt4*, *krt5*, *krt15*, *krt17*, and *krt18)* and skin-regulated genes *(col1a1b*, *cyt1*, and *cki*) from dissected skin tissue on the belly of WT and homozygous *thrab 1-bp insertion (m/m)* mutant fish at larvae (15 dpf) (number of fish = 64–46) and (**B**) at juvenile (28 dpf) stage. The expression of the keratin genes was measured by RT-qPCR as described in Materials and Methods section. The data are expressed as mean ± SE ($n = 3$–6; the p-values are indicated). Two-tail unpaired t-test, p-adjusted <0.05 was used for statistical analysis.

Discussion

In this study, we generated zebrafish in which the *thraa* or *thrab* genes were mutated to understand the deleterious actions of mutant TRα during development. The two C-terminal truncation mutants, ThraaLeu405Glufs*6 or ThrabGlu394*, are similar to those C-terminal truncation mutants identified in patients (Supplementary Fig. S3; see Supplementary Materials and Methods). These two mutants had completely lost T3-binding activity and transcription capacity, and they exhibited dominant negative activity by interfering with the transcription activity of WT TRα1 (Table 2). Furthermore, *in vivo*, the mutants suppressed genes positively regulated by T3 such as the *gh1* gene, and upregulated T3-negatively regulated genes such as the *tshba* gene in the pituitary of homozygous *thrab 1-bp insertion (m/m)* mutant fish. Mutant fish exhibit growth retardation as shown for patients and mice (2,4,5,7,34,35,43). Thus, we have generated a model of RTHα that can be used to interrogate the pathogenic actions of TRα1 mutants during development.

In contrast to humans and mice, in zebrafish the *thra* gene is duplicated. The *thraa* gene encodes two TRα1 isoforms, the long and the short forms. The *thraa 8-bp* insertion site is at nucleotide position 1233 and yields the same truncation mutant protein, ThraaLeu405Glufs*6, for both the long and the short forms (Supplementary Fig. S9A; see Supplementary Materials and Methods). Therefore, for the analysis of the phenotypic expression of *thraa 8-bp ins* fish, one would not need to consider the contribution from the possible actions of the *thraa 8-bp ins* long form variant. The *thrab 1-bp* insertion mutation site was at nucleotide 1180, yielding one single ThrabGlu394* mutant receptor. Therefore, the phenotypic manifestations in these two mutant fish is mediated by either the ThraaLeu405Glufs*6 or the ThrabGlu394* mutant receptor, allowing the comparison of consequences of the mutations in the *thraa* and *thrab* genes. We found that there were both common and distinct actions of these two mutant receptors. Both mutants impaired growth, although the extent of impairment by the homozygous *thrab 1-bp insertion (m/m)* mutant was about fivefold more severe than by the homozygous *thraa 8-bp insertion (m/m)* mutant (Fig. 1; Supplementary Fig. S5; see Supplementary Materials and Methods). The strikingly distinct phenotype in homozygous *thrab 1-bp insertion (m/m)* mutant fish, in contrast to homozygous *thraa 8-bp insertion (m/m)* mutant fish was the appearance of a ''red belly'' due to epidermal hypoplasia (Fig. 4). The homozygous *thrab 1-bp insertion (m/m)* mutant suppresses the expression of a panel of keratin genes at the mRNA and protein levels and inhibits keratinocyte proliferation by attenuating STAT3 signaling to decrease the protein abundance of cell cycle key regulators (Fig. 5C).

At present, it remains unclear how homozygous *thraa 8-bp insertion (m/m)* and homozygous *thrab 1-bp insertion (m/m)* mutants exert differential effects in a tissue-specific manner. Comparison of the primary amino acid sequences shows 96% homology in the DNA-binding domain and 94% in the ligand-binding domain between ThraaLeu405Glufs*6 and ThrabGlu394* mutants (Supplementary Fig. S9A, B; see Supplementary Materials and Methods). The amino A/B domain showed less homology (52%) between these two mutants and furthermore, the *thrab 1-bp insertion* mutant is 16 amino acids shorter at the C-terminus than the *thraa 8-bp insertion* mutant (Supplementary Fig. S9B; see Supplementary Materials and Methods). Previously, using the RTHα mouse model of $Thra1^{PV/+}$ mice, we showed the aberrant interaction of NCOR1 with TRα1 mutants underlying the

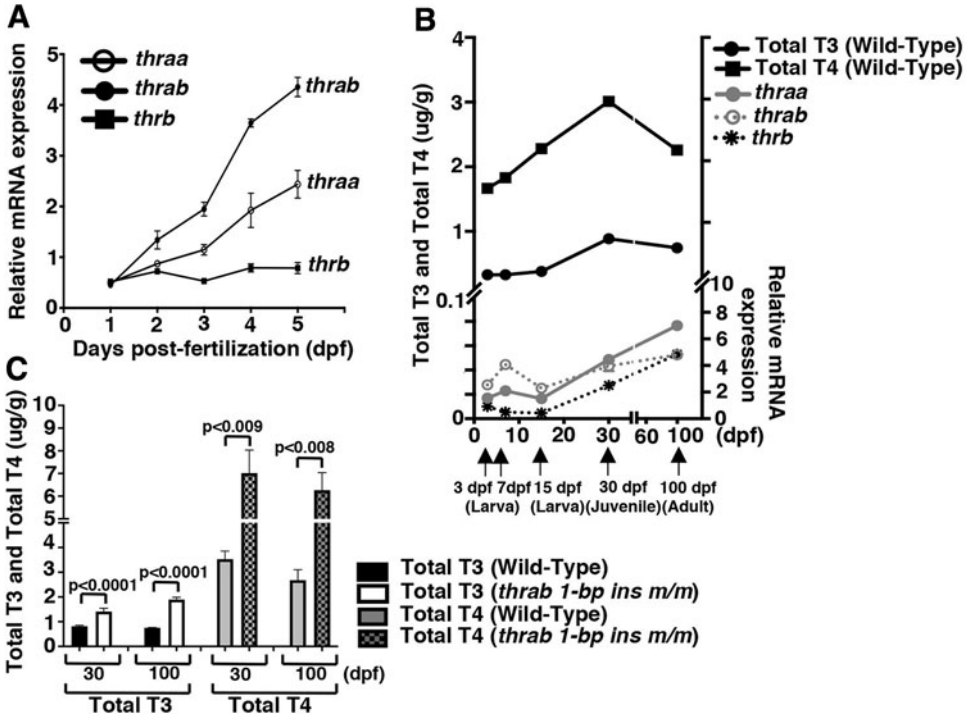

FIG. 7. The whole-body content of thyroid hormones and relative expression patterns of thyroid hormone receptor genes at embryonic, larvae, juvenile, and adult stages. (**A**) Total RNA of pooled embryos or larvae ($N = 25–30$ at each time point from 24 to 120 hpf) were extracted for RT-qPCR analysis. The relative expression of thyroid hormone receptor genes (*thraa*, *thrab*, and *thrb*) were measured and normalized against the housekeeping gene *efla* as described in Materials and Methods section. (**B**) Whole-body content of total L-T4 (TT4) and total L-T3 (TT3) in WT zebrafish were determined from larva to adult at the time point (indicated by the arrows) described in Materials and Methods section. Total RNA of larvae (pooled from 3–7 embryos) or total RNA from skin on the belly of 15-dps larvae, 30-day juveniles or 100-day adults were extracted by RT-qPCR analysis. The relative expression of thyroid hormone receptor genes (*thraa*, *thrab*, and *thrb*) were measured and normalized against the housekeeping gene *efla* as described in Materials and Methods section. For RT-qPCR, the number of whole larvae at 3 and 7 dpf ($N = 25–30$ each), skin on the belly were dissected and extracted at 15 dpf ($N = 35$), at 30 dpf ($N = 15$), and 100 dpf ($N = 10$). The data are shown as mean ± SE ($n = 3$). Whole-body content of TT3 and TT4 are shown as ± SE ($n = 3$). (**C**) Whole-body content of TT3 and TT4 were determined by ELISA in WT and homozygous *thrab 1-bp insertion (m/m)* mutant juvenile at 30 dpf and adult at 100 dpf as described in Materials and Methods section. For 30 dpf juveniles, the number of fish used were in the range of 6–9, or 20–31 per sample, each in triplicates for WT fish and 16–19 or 36 fish per sample, each in triplicates for homozygous *thrab 1-bp ins (m/m)* mutant fish. For 100 dpf adult fish, the number of fish used were 3 per sample, each in triplicates for WT fish and 8–9 or 7–9 fish per sample, each in triplicates for homozygous *thrab 1-bp ins (m/m)* mutants. The data are shown mean ± SE ($n = 6$). Two-tail unpaired *t*-test, *p*-adjusted <0.05 was used for statistical analysis. ELISA, enzyme-linked immunosorbent assay; T3, triiodothyronine, ; T4, thyroxine; TT3, total T3; TT4, total T4.

dominant actions of TRα1 mutants (44). Furthermore, Bochukova *et al.* reported that a patient's mutant was affected by NCOR1 (2), further supporting that constitutive association of NCOR1 with TRα1 mutants could lead to clinical manifestations of RTHα. Therefore, it is reasonable to speculate that the *thrab 1-bp insertion* mutant in which the C-terminal T3-binding domain is 16-amino acids shorter, could lead to a stronger interaction than the *thraa 8-bp insertion* mutant with the co-repressor complexes, leading to distinct and more severe phenotypes. However, it is not possible to fully understand the molecular basis of the observed differential activity, especially in a target tissue-dependent manner of these duplicated gene mutants, owing to the lack of detailed crystal structure information. Nevertheless, this question warrants further studies in the future.

Previously, using a morpholino approach, Marelli *et al.* demonstrated that morphants expressing dominant negative *thraa* exhibit severe developmental abnormalities in embryos and in the embryo–larva transition (13). The phenotypes of *thraa*-morphants showed brain and cardiac defects, but with normal *tshba* expression. Furthermore, embryos injected with several human *THRA* mutants to express the mutant receptors ectopically also manifested variable defects, including cerebral and cardiac edema, incomplete formation of the vascular network, and abnormal motoneurons and craniofacial development (14). In contrast to these findings, we did not detect any discernible morphological abnormalities in the embryos and early larvae in homozygous *thrab 1-bp insertion (m/m)* and homozygous *thraa 8-bp insertion (m/m)* mutant fish. Our close evaluation found that mutant embryos developed similarly as in sibling WT embryos. The first visible abnormal development was a hypoplastic epidermis at the larva–juvenile transition (28 dpf) of homozygous *thrab 1-bp insertion (m/m)* fish with the appearance of a ''red belly,'' which persisted to adulthood. We detected growth impairment of homozygous *thrab 1-bp insertion (m/m)* mutant fish only in the larva–juvenile transition beginning at 28 dpf, which persisted to adulthood. It is not immediately clear what may account for

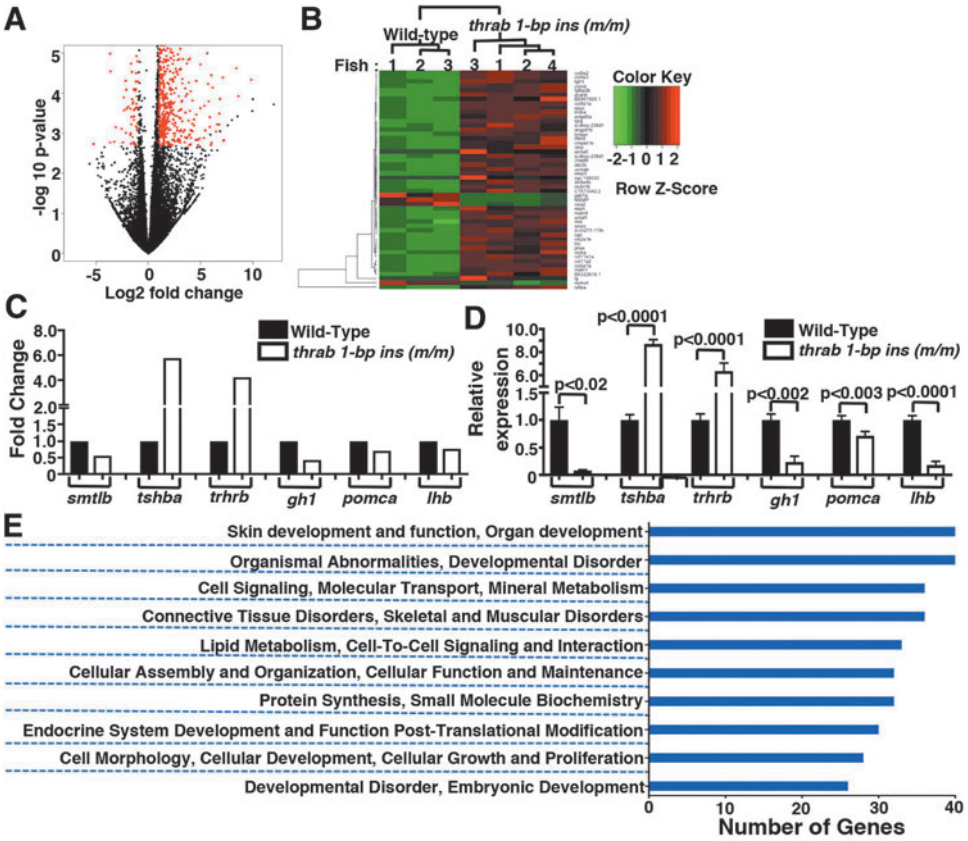

FIG. 8. Global impact on the gene expression profile and biological processes of the pituitary by female homozygous *thrab 1-bp insertion (m/m)* mutant fish. Total RNA was isolated from pituitaries of WT ($n=3$) and homozygous *thrab 1-bp insertion (m/m)* mutant fish ($n=4$) for transcriptome analysis. (**A**) The genes marked in red in this volcano plot were significantly expressed genes with fold changes ≥2 and FDR ≤0.05. The total number of differentially expressed genes was 723, with 642 genes upregulated and 81 genes downregulated. (**B**) A heatmap presentation of hierarchical clustering analysis of top 50 expressed genes selected by FDR from the significant gene list (fold changes ≥2 and FDR ≤0.05). (**C**) Comparison of the gene expression profiles of major pituitary hormone transcripts (*smtlb*, *tshba*, *trhrb*, *gh1*, *pomca*, and *lhb*) in the pituitary of WT and homozygous *thrab 1-bp insertion (m/m)* mutant fish. (**D**) The mRNA expression levels of the major pituitary hormone transcripts (*smtlb*, *tshba*, *trhrb*, *gh1*, *pomca*, and *lhb*) were measured by RT-qPCR in pituitaries of WT and homozygous *thrab 1-bp insertion (m/m)* mutant fish (number of fish = 46–62, number of determinations = 3–6). The data are shown as mean ± SE with *p*-values to indicate significant changes. Two-tail unpaired *t*-test, *p*-adjusted <0.05 was used for statistical analysis. (**E**) Graphical representation of clusters of biological processes with Gene Ontology analysis for the significantly expressed genes. FDR, false discovery rate.

the difference between the findings reported by Marelli *et al.* (13,14) and the findings presented in this study. One possibility could be the different methodologies used to induce the expression of mutants in the embryos of zebrafish, and possibly differences in the expression levels of the mutants.

In this study, we used CRISPR/Cas9-mediated targeted mutagenesis to create the mutations of the two *thra* duplicated genes. This method allowed us to study the expression of mutant receptors by using endogenous promoters and transcription regulatory systems in the physiological context. The stable expression of mutant receptors facilitated the analysis of the actions of mutant receptors from embryos to adulthood. Consistent with reports by others (13,45,46), we found that *thraa*, *thrab*, and *thrb* are expressed in the embryos (Fig. 7A, B). While all TR genes are expressed, the *thrab* gene is the most abundant among the three genes during embryonic development (Fig. 7A, B). However, we found that homozygous mutations of either the *thraa* or *thrab* gene did not affect embryonic/larva development and larva transition in the mutant fish. One possible explanation for a lack of abnormalities in the embryonic development by mutation of the *thraa* or *thrab* gene could be the compensatory functions of other unaffected receptors to overcome the deleterious actions of mutant receptors. However, such compensatory mechanisms could not fully explain the phenotypes of impaired growth and hypoplastic epidermis emerging at the larva–juvenile transition and persisting to adulthood. One plausible alternative mechanism could be the temporal signaling mediated by thyroid hormones. As shown in Figure 7B, TT3 and TT4 were relatively low in the embryonic stage, suggesting that the WT TRs were most likely unliganded. Thus, there was not sufficient ligand-dependent transcription activity of WT receptors to be interfered/antagonized by mutant receptors, which cannot bind thyroid hormones. As the levels of TT3 and TT4 began to rise on day 15 and peaked at the larva–juvenile transition at day 30, more WT TRs are expected to be bound by thyroid hormones in WT fish, particularly in homozygous *thrab 1-bp insertion (m/m)* mutant fish, in which TT3 and TT4 were higher than WT fish at 30 and 100 dpf (elevated 1.7- to 2.5-fold; Fig. 7C). However, the homozygous *thrab 1-bp insertion (m/m)* mutant,

which cannot bind thyroid hormone, would act in a dominant negative manner to interfere with the transcriptional activity on the T3-target genes. This possibility was supported by the findings that the expression of *keratin-4*, *keratin-17*, and *keratin-18* was not affected as shown by whole mount *in situ* hybridization (WISH) between days 1 and 5 during in embryos and the embryo–larva transition (Supplementary Fig. S10B–D; see Supplementary Materials and Methods), but was suppressed in juveniles (Fig. 6) and adults (Fig. 5), thus leading to epidermal hypoplasia. Similarly, there were no changes in the expression of the *gh1* gene as shown by WISH in Day 2 to Day 5 embryos and the embryo–larva transition (Supplementary Fig. S10A; see Supplementary Materials and Methods; no *gh1* expression was detected on day 1), but the *gh1* gene expression was suppressed in juveniles (Fig. 3) and adults (Fig. 2), thus leading to growth impairment. These results underscore the critical role of thyroid hormone in directing the developmental program of zebrafish. Indeed, the demonstration that the rise of TT3 and TT4 at the larva–juvenile transition is critical for postlarval growth shown in this study (Fig. 7B) is consistent with the findings in mice and *Xenopus tropicalis*. In WT mice, serum TT3 and TT4 are not detectable on the day of birth and rise to reach a peak on P15 (42). In athyroid *Pax8*$^{-/-}$ mice, the fetus develops and pups are born at term, but if without treatment with thyroid hormone postnatally, the pups die around weaning (47). In *X. tropicalis*, plasma T3 and T4 are not detectable in early tadpoles, and begin to rise at the premetamorphosis stages 55 and 57, respectively, and reach a peak at metamorphosis climax (stages 61 and 62 for T3 and T4, respectively) for transition and for post-metamorphosis growth (48).

The observation that TT3 and TT4 are relatively low in the embryos and early larvae (3–7 dpf; Fig. 7B) suggests that liganded TRs may not be critical in the initiation of embryogenesis of zebrafish. This notion is supported by the observations that the total absence of thyroid hormone in athyroid *Pax8*$^{-/-}$ mice did not prevent the development of pups to term, although the pups die shortly after weaning unless supplemented with thyroid hormones (47). In athyroid *Pax8*$^{-/-}$ mice, TRs are expressed, but mice develop to term, suggesting that liganded TR is not required in the initiation of development. Furthermore, Gothe *et al.* reported that mice devoid of all known TRs develop to term and remain viable long enough to reach adulthood. Mice deficient in all known TRs, however, exhibit postnatal disorders in several target organs, such as retarded growth and delayed bone maturation (49). Given the observations that pups were born at term in athyroid *Pax8*$^{-/-}$ mice, as well as in mice deficient in all known TRs, we suggest that TRs might not be required to initiate the development program in zebrafish as mutations of the two duplicated *thra* genes do not result in any discernable abnormalities during embryogenesis. However, the *thrab* gene is clearly essential for postlarval growth and the development of certain specific tissues such as the skin. Recently, Yuki *et al.* (pers. comm.) found that *X. tropicalis* tadpoles deficient in both TRα and TRβ (double knockout tadpoles) are able to initiate metamorphosis and accomplish many metamorphic changes, such as limb development. But double knockout tadpoles stall and eventually die soon after reaching stage 61, the climax of metamorphosis. The authors concluded that TRs are not required for the initiation of metamorphosis but are essential for the completion of metamorphosis and subsequent survival. Unlike in mice, the transparent zebrafish embryos that develop outside of the body allowed us to clearly visualize possible defects during development, thus providing direct evidence in support of the notion that TRs might not be required in initiating development of zebrafish embryos. Thus, our findings demonstrate the conserved role of TRs in postembryonic development and homeostasis in mice, *Xenopus*, and zebrafish.

This study shows that the expression of the *tshba* gene is elevated at the mRNA level (Fig. 8C, D) accompanied by elevated TT3 and TT4 levels (Fig. 7C) in *homozygous 1-bp insertion (m/m)* mutant fish. Currently, it is not possible to determine the serum TSH concentrations in zebrafish. However, if the elevated *tshba* mRNA were to be linearly translated into TSH polypeptide in the pituitary and secreted out of the pituitary, it would seem that *homozygous 1-bp insertion (m/m)* mutant fish would exhibit elevated T3, T4, and TSH profiles. In RTHα patients, serum T3 can be high-normal to high, T4 normal to low, while TSH is normal or mildly raised (22). Thus, except for T4, it would seem that T3 and TSH levels would be in concordance with those observed in RTHα patients. At present, the molecular basis for the minor hormonal profile differences between RTHα patients and mutant zebrafish is not clear.

As in patients and mice with mutations of TRα1, zebrafish expressing mutated *thraa* and *thrab* genes exhibit postembryonic growth retardation, indicating the conserved role of TRα1 in growth regulation among these three species. Interestingly, patients with mutations of TRα1 were reported to exhibit a skin disorder with skin tags (34). At present, it is not clear how the skin tags found in patients with mutations of TRα1 may be related to the hypoplastic epidermis found in homozygous *thrab 1-bp insertion (m/m)* mutant fish. Nonetheless, the skin tags found in patients would suggest that TRα1 mutations would impact skin biology in patients. Indeed, skin is the largest organ of the human body and serves as a barrier to protect the individual from external insults. Thyroid hormone is known to directly affect cutaneous biology, including the epidermis, dermis, and hair. All three T3-binding TR isoforms have been identified in skin tissues (50,51). TRs were shown to directly regulate gene expression in the skin (37). Hypothyroid patients have pale, cold, dry, and xerotic skin with thin epidermis (52). Hypothyroidism at the tissue level is either caused by decreased cellular levels of thyroid hormone or caused by resistance of target tissues to hormone action. This study shows that mutations of the *thrab* gene lead to epidermal hypoplasia with an easily recognizable phenotype (''red belly'') as early as 4 weeks postfertilization. Thus, this zebrafish model is an excellent tool to further elucidate the actions of TRs, and for rapid screening of potential therapeutics for treating skin disorders.

Acknowledgments

We thank Dr. Luca Persani (Universita degli Studi di Milano, Italy) for the generous gift of *zthraaL* plasmid. To make probes for WISH analyses, we are grateful to Dr. Driever Wolfgang (Albert-Ludwigs-University Freiburg, Germany) for keratin-4, keratin-5, and keratin-17 plasmids; Dr. Benzamin Feldman (NIH/NICHD, USA) for keratin-4, keratin-8, and keratin-18 plasmids; Dr. Eric C. Liao (Harvard University, USA) for keratin-4 and keratin-18 plasmids; Dr. Hammerschmidt Matthias (University of Cologne, Germany) and Dr. David Kimelman (University of Washington, USA) for the p63 plasmid; and Dr. Alberto Rissone (NIH/NHGRI, USA) for the gh1 probe. We thank Dr. Alberto Rissone and Dr. Erica Bresciani

(NIH/NHGRI, USA) for valuable discussions and for teaching us WISH, and Dr. Peter McPhie for the analysis of T3-binding data. We also thank Ross Lake (NIH/LGCP Microscopy Core Facility) for discussion of and suggestions for our study. We are indebted to Dr. Victoria Hoffmann (Division of Veterinary Resources, Diagnostic and Research Services Branch, NIH) for showing us how to dissect the tiny pituitary from zebrafish.

Author Disclosure Statement

The authors declare no conflicts of interest.

Funding Information

This research was supported by the Intramural Research Program (InnovationAward) of the Center for Cancer Research, National Cancer Institute, and National Institutes of Health.

Supplementary Material

Supplementary Materials and Methods
Supplementary Table S1
Supplementary Table S2
Supplementary Table S3
Supplementary Figure S1
Supplementary Figure S2
Supplementary Figure S3
Supplementary Figure S4
Supplementary Figure S5
Supplementary Figure S6
Supplementary Figure S7
Supplementary Figure S8
Supplementary Figure S9
Supplementary Figure S10

References

1. Concolino P, Costella A, Paragliola RM 2019 Mutational landscape of resistance to thyroid hormone beta (RTHbeta). Mol Diagn Ther **23:**353–368.
2. Bochukova E, Schoenmakers N, Agostini M, Schoenmakers E, Rajanayagam O, Keogh JM, Henning E, Reinemund J, Gevers E, Sarri M, Downes K, Offiah A, Albanese A, Halsall D, Schwabe JW, Bain M, Lindley K, Muntoni F, Vargha-Khadem F, Dattani M, Farooqi IS, Gurnell M, Chatterjee K 2012 A mutation in the thyroid hormone receptor alpha gene. N Engl J Med **366:**243–249.
3. van Mullem AA, Chrysis D, Eythimiadou A, Chroni E, Tsatsoulis A, de Rijke YB, Visser WE, Visser TJ, Peeters RP 2013 Clinical phenotype of a new type of thyroid hormone resistance caused by a mutation of the TRalpha1 receptor: consequences of LT4 treatment. J Clin Endocrinol Metab **98:**3029–3038.
4. Moran C, Schoenmakers N, Agostini M, Schoenmakers E, Offiah A, Kydd A, Kahaly G, Mohr-Kahaly S, Rajanayagam O, Lyons G, Wareham N, Halsall D, Dattani M, Hughes S, Gurnell M, Park SM, Chatterjee K 2013 An adult female with resistance to thyroid hormone mediated by defective thyroid hormone receptor alpha. J Clin Endocrinol Metab **98:**4254–4261.
5. Tylki-Szymanska A, Acuna-Hidalgo R, Krajewska-Walasek M, Lecka-Ambroziak A, Steehouwer M, Gilissen C, Brunner HG, Jurecka A, Rozdzynska-Swiatkowska A, Hoischen A, Chrzanowska KH 2015 Thyroid hormone resistance syndrome due to mutations in the thyroid hormone receptor alpha gene (THRA). J Med Genet **52:**312–316.
6. Moran C, Agostini M, McGowan A, Schoenmakers E, Fairall L, Lyons G, Rajanayagam O, Watson L, Offiah A, Barton J, Price S, Schwabe J, Chatterjee K 2017 Contrasting phenotypes in resistance to thyroid hormone alpha correlate with divergent properties of thyroid hormone receptor alpha1 mutant proteins. Thyroid **27:**973–982.
7. Kaneshige M, Suzuki H, Kaneshige K, Cheng J, Wimbrow H, Barlow C, Willingham MC, Cheng S 2001 A targeted dominant negative mutation of the thyroid hormone alpha 1 receptor causes increased mortality, infertility, and dwarfism in mice. Proc Natl Acad Sci U S A **98:**15095–15100.
8. O'Shea PJ, Harvey CB, Suzuki H, Kaneshige M, Kaneshige K, Cheng SY, Williams GR 2003 A thyrotoxic skeletal phenotype of advanced bone formation in mice with resistance to thyroid hormone. Mol Endocrinol **17:** 1410–1424.
9. Bassett JH, Boyde A, Zikmund T, Evans H, Croucher PI, Zhu X, Park JW, Cheng SY, Williams GR 2014 Thyroid hormone receptor alpha mutation causes a severe and thyroxine-resistant skeletal dysplasia in female mice. Endocrinology **155:**3699–3712.
10. Park S, Han CR, Park JW, Zhao L, Zhu X, Willingham M, Bodine DM, Cheng SY 2017 Defective erythropoiesis caused by mutations of the thyroid hormone receptor alpha gene. PLoS Genet **13:**e1006991.
11. Darras VM, Van Herck SL, Heijlen M, De Groef B 2011 Thyroid hormone receptors in two model species for vertebrate embryonic development: chicken and zebrafish. J Thyroid Res **2011:**402320.
12. Takayama S, Hostick U, Haendel M, Eisen J, Darimont B 2008 An F-domain introduced by alternative splicing regulates activity of the zebrafish thyroid hormone receptor alpha. Gen Comp Endocrinol **155:**176–189.
13. Marelli F, Carra S, Agostini M, Cotelli F, Peeters R, Chatterjee K, Persani L 2016 Patterns of thyroid hormone receptor expression in zebrafish and generation of a novel model of resistance to thyroid hormone action. Mol Cell Endocrinol **424:**102–117.
14. Marelli F, Carra S, Rurale G, Cotelli F, Persani L 2017 *In vivo* functional consequences of human THRA variants expressed in the zebrafish. Thyroid **27:**279–291.
15. Kimmel CB, Ballard WW, Kimmel SR, Ullmann B, Schilling TF 1995 Stages of embryonic development of the zebrafish. Dev Dyn **203:**253–310.
16. Varshney GK, Carrington B, Pei W, Bishop K, Chen Z, Fan C, Xu L, Jones M, LaFave MC, Ledin J, Sood R, Burgess SM 2016 A high-throughput functional genomics workflow based on CRISPR/Cas9-mediated targeted mutagenesis in zebrafish. Nat Protoc **11:**2357–2375.
17. Sood R, Carrington B, Bishop K, Jones M, Rissone A, Candotti F, Chandrasekharappa SC, Liu P 2013 Efficient methods for targeted mutagenesis in zebrafish using zinc-finger nucleases: data from targeting of nine genes using CompoZr or CoDA ZFNs. PLoS One **8:**e57239.
18. McMenamin SK, Bain EJ, McCann AE, Patterson LB, Eom DS, Waller ZP, Hamill JC, Kuhlman JA, Eisen JS, Parichy DM 2014 Thyroid hormone-dependent adult pigment cell lineage and pattern in zebrafish. Science **345:**1358–1361.
19. Li B, Dewey CN 2011 RSEM: accurate transcript quantification from RNA-Seq data with or without a reference genome. BMC Bioinformatics **12:**323.
20. Robinson MD, McCarthy DJ, Smyth GK 2010 edgeR: a Bioconductor package for differential expression analysis of digital gene expression data. Bioinformatics **26:**139–140.

21. Zhu X, Zhu YJ, Kim DW, Meltzer P, Cheng SY 2014 Activation of integrin-ERBB2 signaling in undifferentiated thyroid cancer. Am J Cancer Res **4:**776–788.
22. van Gucht ALM, Moran C, Meima ME, Visser WE, Chatterjee K, Visser TJ, Peeters RP 2017 Resistance to thyroid hormone due to heterozygous mutations in thyroid hormone receptor alpha. Curr Top Dev Biol **125:**337–355.
23. Marelli F, Persani L 2018 Role of TRs in zebrafish development. Methods Mol Biol **1801:**287–298.
24. Tinnikov A, Nordstrom K, Thoren P, Kindblom JM, Malin S, Rozell B, Adams M, Rajanayagam O, Pettersson S, Ohlsson C, Chatterjee K, Vennstrom B 2002 Retardation of post-natal development caused by a negatively acting thyroid hormone receptor alpha1. Embo J **21:**5079–5087.
25. Wood DF, Franklyn JA, Docherty K, Ramsden DB, Sheppard MC 1987 The effect of thyroid hormones on growth hormone gene expression *in vivo* in rats. J Endocrinol **112:**459–463.
26. Kamegai J, Tamura H, Ishii S, Sugihara H, Wakabayashi I 2001 Thyroid hormones regulate pituitary growth hormone secretagogue receptor gene expression. J Neuroendocrinol **13:**275–278.
27. Marchand O, Duffraisse M, Triqueneaux G, Safi R, Laudet V 2004 Molecular cloning and developmental expression patterns of thyroid hormone receptors and T3 target genes in the turbot (*Scophtalmus maximus*) during post-embryonic development. Gen Comp Endocrinol **135:**345–357.
28. Fukamachi S, Yada T, Mitani H 2005 Medaka receptors for somatolactin and growth hormone: phylogenetic paradox among fish growth hormone receptors. Genetics **171:** 1875–1883.
29. Astola A, Pendon C, Ortiz M, Valdivia MM 1996 Cloning and expression of somatolactin, a pituitary hormone related to growth hormone and prolactin from gilthead seabream, Sparus aurata. Gen Comp Endocrinol **104:**330–336.
30. Velloso CP 2008 Regulation of muscle mass by growth hormone and IGF-I. Br J Pharmacol **154:**557–568.
31. Fuentes EN, Valdes JA, Molina A, Bjornsson BT 2013 Regulation of skeletal muscle growth in fish by the growth hormone—insulin-like growth factor system. Gen Comp Endocrinol **192:**136–148.
32. Roberts SB, McCauley LA, Devlin RH, Goetz FW 2004 Transgenic salmon overexpressing growth hormone exhibit decreased myostatin transcript and protein expression. J Exp Biol **207:**3741–3748.
33. Schiaffino S, Mammucari C 2011 Regulation of skeletal muscle growth by the IGF1-Akt/PKB pathway: insights from genetic models. Skelet Muscle **1:**4.
34. Moran C, Agostini M, Visser WE, Schoenmakers E, Schoenmakers N, Offiah AC, Poole K, Rajanayagam O, Lyons G, Halsall D, Gurnell M, Chrysis D, Efthymiadou A, Buchanan C, Aylwin S, Chatterjee KK 2014 Resistance to thyroid hormone caused by a mutation in thyroid hormone receptor (TR)alpha1 and TRalpha2: clinical, biochemical, and genetic analyses of three related patients. Lancet Diabetes Endocrinol **2:**619–626.
35. Demir K, van Gucht AL, Buyukinan M, Catli G, Ayhan Y, Bas VN, Dundar B, Ozkan B, Meima ME, Visser WE, Peeters RP, Visser TJ 2016 Diverse genotypes and phenotypes of three novel thyroid hormone receptor-alpha mutations. J Clin Endocrinol Metab **101:**2945–2954.
36. Slominski A, Wortsman J 2000 Neuroendocrinology of the skin. Endocr Rev **21:**457–487.
37. Antonini D, Sibilio A, Dentice M, Missero C 2013 An intimate relationship between thyroid hormone and skin: regulation of gene expression. Front Endocrinol (Lausanne) **4:**104.
38. Macias E, Rao D, Digiovanni J 2013 Role of stat3 in skin carcinogenesis: insights gained from relevant mouse models. J Skin Cancer **2013:**684050.
39. Miyoshi K, Takaishi M, Nakajima K, Ikeda M, Kanda T, Tarutani M, Iiyama T, Asao N, DiGiovanni J, Sano S 2011 Stat3 as a therapeutic target for the treatment of psoriasis: a clinical feasibility study with STA-21, a Stat3 inhibitor. J Invest Dermatol **131:**108–117.
40. Sano S, Chan KS, DiGiovanni J 2008 Impact of Stat3 activation upon skin biology: a dichotomy of its role between homeostasis and diseases. J Dermatol Sci **50:**1–14.
41. Buettner R, Mora LB, Jove R 2002 Activated STAT signaling in human tumors provides novel molecular targets for therapeutic intervention. Clin Cancer Res **8:**945–954.
42. Friedrichsen S, Christ S, Heuer H, Schafer MK, Mansouri A, Bauer K, Visser TJ 2003 Regulation of iodothyronine deiodinases in the $Pax8^{-/-}$ mouse model of congenital hypothyroidism. Endocrinology **144:**777–784.
43. Espiard S, Savagner F, Flamant F, Vlaeminck-Guillem V, Guyot R, Munier M, d'Herbomez M, Bourguet W, Pinto G, Rose C, Rodien P, Wemeau JL 2015 A novel mutation in THRA gene associated with an atypical phenotype of resistance to thyroid hormone. J Clin Endocrinol Metab **100:**2841–2848.
44. Fozzatti L, Kim DW, Park JW, Willingham MC, Hollenberg AN, Cheng SY 2013 Nuclear receptor corepressor (NCOR1) regulates *in vivo* actions of a mutated thyroid hormone receptor alpha. Proc Natl Acad Sci U S A **110:**7850–7855.
45. Lazcano I, Rodriguez-Ortiz R, Villalobos P, Martinez-Torres A, Solis-Sainz JC, Orozco A 2019 Knock-down of specific thyroid hormone receptor isoforms impairs body plan development in zebrafish. Front Endocrinol (Lausanne) **10:**156.
46. Liu YW, Chan WK 2002 Thyroid hormones are important for embryonic to larval transitory phase in zebrafish. Differentiation **70:**36–45.
47. Mansouri A, Chowdhury K, Gruss P 1998 Follicular cells of the thyroid gland require Pax8 gene function. Nat Genet **19:**87–90.
48. Leloup J, Buscaglia M 1977 La triiodothyronine: hormone de la metamorphose desamphibiens. C R Acad Sci **284:** 2261–2263.
49. Gothe S, Wang Z, Ng L, Kindblom JM, Barros AC, Ohlsson C, Vennstrom B, Forrest D 1999 Mice devoid of all known thyroid hormone receptors are viable but exhibit disorders of the pituitary-thyroid axis, growth, and bone maturation. Genes Dev **13:**1329–1341.
50. Ahsan MK, Urano Y, Kato S, Oura H, Arase S 1998 Immunohistochemical localization of thyroid hormone nuclear receptors in human hair follicles and *in vitro* effect of L-triiodothyronine on cultured cells of hair follicles and skin. J Med Invest **44:**179–184.
51. Billoni N, Buan B, Gautier B, Gaillard O, Mahe YF, Bernard BA 2000 Thyroid hormone receptor beta1 is expressed in the human hair follicle. Br J Dermatol **142:**645–652.
52. Kasumagic-Halilovic E 2014 Thyroid disease and the skin. Ann Thyroid Res **1:**27–31.

Address correspondence to:
Sheue-yann Cheng, PhD
Laboratory of Molecular Biology
National Cancer Institute
National Institutes of Health
37 Convent Drive, Room 5128
Bethesda, MD 20892-4264

E-mail: chengs@mail.nih.gov